PERGAMON

Archives of Oral Biology 45 (2000) 237–245

Archives of Oral Biology

www.elsevier.com/locate/archoralbio

Distribution of plasma-membrane Ca^{2+} pump in mandibular condyles from growing and adult rabbits

Mohamed M. Sharawy[a,*], Ki.-Ho Kang[a], Kyung.-Wook Kim[b], James L. Borke[a]

[a]*Department of Oral Biology & Maxillofacial Pathology, Medical College of Georgia, School of Dentistry, Augusta, GA 30912, USA*
[b]*Department of Oral & Maxillofacial Surgery, Dankook University, School of Dentistry, Sindbudog, Cheonan, South Korea*

Accepted 8 August 1999

Abstract

Chondrocytes may control the mineralization of the extracellular matrix of condylar cartilage by several mechanisms including the release of microvesicles involved in the initial nucleation, the creation or modification of the local matrix to help propagate or restrict mineralization, and the regulation of the ionic environment at the calcifying foci within the matrix. The plasma membrane Ca^{2+}–Mg^{2+} ATPase (Ca^{2+} pump) is known to play a part in the vectorial efflux of calcium in a variety of cells including chondrocytes. The purpose here was to study the distribution of Ca^{2+}-pump protein in mandibular condyles from growing and adult rabbits, and compare the expression of that protein in progressively differentiating chondrocytes whose final stage is associated with a mineralized extracellular matrix. Ca^{2+}-pump antigen was identified immunohistochemically in six growing and six adult rabbit mandibular condyles with a Ca^{2+} pump-specific monoclonal antibody. The presence of Ca^{2+}-pump antigen was established in hypertrophic chondrocytes, and in osteoblasts and osteoclasts of subchondral bone. Slot-blot analysis of nitrocellulose-immobilized chondrocyte homogenates showed that the amount of Ca^{2+} pump in growing cartilage was more than twice that in adult cartilage ($p < 0.05$). The demonstration of Ca^{2+}-pump antigen in the hypertrophic chondrocytes of growing rabbit condyles is consistent with a role for the plasma-membrane Ca^{2+} pump in the calcification of mandibular condylar cartilage.

Keywords: Ca^{2+} pump; Cartilage; Calcification

1. Introduction

Endochondral bone formation occurs at several sites in the body including the base of the skull and the mandible. It begins as cartilage cells differentiate from mesenchymal cells, and proceeds rapidly via matrix secretion, rapid cell growth and differentiation. As cartilage differentiation proceeds, the cells organize into columns of three functionally distinct zones: the zone of proliferation, the zone of hypertrophy and maturation, and the zone of provisional mineralization (Ten Cate, 1998). In the zone of hypertrophy and maturation, the chondroblast increases in size and secretes mostly proteoglycans. As the maximum size of the chondroblast is reached, type X collagen, chondrocal-

Abbreviations: DAB, 3; 3′-diaminobenzidine tetrahydrochloride; PBS, phosphate-buffered saline; SDS–PAGE, sodium dodecyl sulphate–polyacrylamide gel electrophoresis.

* Corresponding author. Tel. +1-706-721-2526; fax: +1-706-721-6276.

E-mail address: msharawy@mail.mcg.edu (M.M. Sharawy).

0003-9969/00/$ - see front matter
PII: S0003-9969(99)00126-0

cin and bone sialoprotein are produced and together create an environment, which, under the appropriate conditions, can mineralize. When mineralization does occur it does so following the production of matrix vesicles (Ten Cate, 1998).

During cartilage calcification there is an influx of a large amount of Ca^{2+} into cells in the hypertrophic cell zone of the mandibular condyle and growth plate (Matthews and Martin, 1971; Ianotti et al., 1985; Gunter et al., 1990). This influx requires an intracellular Ca^{2+}-regulating system to protect cells from the influx.

Calcium enters chondrocytes and most other cells through Ca^{2+} channels down a concentration gradient from an external Ca^{2+} concentration of approx. 10^{-3}M to an intracellular concentration of approx. 10^{-7}M. Studies by Balmain et al. (1989, 1993) have clearly shown that the localization of calbindin D9 K, a vitamin D-dependent calcium-binding protein known to play a part in the transport of calcium across the cytosol of Ca^{2+}-transporting tissues, and 1,25 dihydroxyvitamin D_3 receptors are both found in high abundance in chondrocytes from zones of matrix vesicle calcification.

This localization corresponds in cartilage with Ca^{2+}–Mg^{2+} ATPase activity in the plasma membrane of chondrocytes, suggesting a role for the plasma-membrane Ca^{2+} pump in the calcification of cartilage (Akisaka and Gay, 1985). The techniques generally used to measure Ca^{2+}–Mg^{2+} ATPase activity have limitations in their ability to distinguish Ca^{2+}-pump activity from either ecto-ATPases, which are not involved with Ca^{2+} transport, or from other membrane phosphatases (Moy et al., 1986; Stahl and Baskin, 1990). The use of a monoclonal antibody directed against the Ca^{2+}–Mg^{2+} ATPase pump (Borke et al., 1989) may provide more precise information on how calcium transport is regulated in chondrocytes of the mandibular condylar cartilage.

Recent studies have postulated an active role for chondrocytes in biological cartilage calcification (Cowell et al., 1987; Anderson, 1992; Hunziker, 1994). The chondrocytes appear to regulate all phases of mineralization: by producing matrix vesicles, which are thought to be the initial nucleation sites for calcification; by creating and modifying the local matrix composition by secreting several types of collagens; and by regulating the ionic environment at the mineralization foci. The exact mechanism of each process is still under investigation.

In addition to the Ca^{2+}–Mg^{2+} ATPase pump, mitochondria have been suggested as another regulating system for intracellular Ca^{2+} homeostasis (Lehninger, 1978; Carafoli, 1987). Mitochondrial Ca^{2+} accumulation and its release appear to be associated with initial calcification in growth-plate cartilage, such as the initial nucleation of apatite crystals within matrix vesicles (Brighton and Hunt, 1974). How mitochondria transport accumulated calcium or calcium phosphate granules through the plasma membrane into the matrix, and how matrix vesicles accumulate large amounts of calcium for initial nucleation in biological cartilage calcification remain unknown. Therefore, localization of the plasma-membrane Ca^{2+} pump may suggest a mechanism by which chondrocytes regulate Ca^{2+} movement in relation to the initial calcification of cartilage. We have now sought to study the distribution of Ca^{2+}-pump protein in chondrocytes of the rabbit condyler cartilage.

2. Materials and methods

2.1. Light-microscopic immunohistochemistry

2.1.1. Animals

Three growing (1–1.5 kg) and three adult (4–4.5 kg) New Zealand male rabbits (*Oryctolagus cuniculus*) were deeply anaesthetized and perfused intracardially with saline containing 100 units/ml heparin and 2% formaldehyde for light-microscopic immunohistochemistry. The research protocol was approved by the Medical College of Georgia Animal Use for Research and Education Committee and followed the highest principles of animal welfare.

Each rabbit was first anaesthetized by injection of a mixture of Rompun (xylazine, 50 mg/kg) and Ketaset (ketamine HC1, 250 mg/kg) into the muscles of the hind leg. Under deep anaesthesia, an infusion pump was used to deliver the fixative solution through the heart into the systemic circulation at a rate similar to the rabbit cardiac output. A total of 400 ml of normal saline solution containing heparin (1000 units/ml) was infused to prevent blood coagulation, followed by infusion of 400 ml of the fixative solution. The fixed mandibular condyles were dissected quickly and placed for 2 h in fresh 2% formaldehyde for rapid stabilization.

2.1.2. Paraffin-embedded sections

The fixed condyles were demineralized in 4% EDTA, pH 7.2–7.4, at 4°C for 4–6 weeks, then washed under running water for several hours. They were then cut sagittally and horizontally with a scalpel under the microscope and the tissue segments were dehydrated through a series of ethanols and xylenes. The segments were then embedded in paraffin blocks for serial sectioning and cut along the sagittal or horizontal plane for immunohistochemical labelling.

2.1.3. Immunohistochemical labelling and quantitation of Ca^{2+} pump

The monoclonal antibody 5F10 (Sigma, St. Louis,

MO) directed against the plasma-membrane Ca^{2+} pump that was used for immunohistochemical and Western blotting procedures was first described by Borke et al. (1989). It was prepared by cell fusion and hybridoma selection and shown to recognize a membrane-spanning region on the erythrocyte Ca^{2+}-pump molecules in a wide range of tissues and species.

Serial sections of the condyles were processed for immunohistochemical localization of plasma-membrane Ca^{2+}-pump epitopes using the avidin–biotin–peroxidase technique of Hsu et al. (1981). In this technique, the tissue sections were deparaffinized with D-limonene (Sigma) and rehydrated through a graded series of ethanols before being placed in PBS, pH 7.4. They were then incubated in 3% hydrogen peroxide for 10 min to block endogenous peroxidase activity. After rinsing with PBS, sections were incubated in 10 mg/ml bovine serum albumin (Sigma) in PBS for 1 h to block non-specific binding of the secondary antibodies. The sections were next incubated in a 1:750 dilution of the monoclonal antibody 5F10 for 1 h, followed by rinsing with PBS. They were next incubated in a 1:200 dilution of a biotinylated horse anti-mouse IgG (Vector Laboratories, Burlingame, CA) for 30 min and rinsed with PBS. Avidin–peroxidase complex (ABC™ Reagent; Vector) was applied and the sections incubated for 30 min. Following incubation, the sections were rinsed thoroughly with two changes of PBS, and incubated in a peroxidase substrate solution containing 0.05 M DAB, (Sigma) and 0.03% hydrogen peroxide in PBS. The reaction was monitored under the microscope and stopped after 2–10 min with sterile water.

Following immunohistochemical processing, some of the sections were counterstained with Mayer's haematoxylin (Sigma) to aid in morphological identification. Sections of rat kidney known to contain 5F10-reactive Ca^{2+}-pump epitopes were processed as positive controls. Serial sections were also simultaneously processed as negative controls without incubation in the primary antibody 5F10.

Each photomicrograph of these negative control sections was placed with that of experimental sections. The immunostaining intensity and distribution in experimental sections were compared to those in control sections and scored on a scale of "0" to "+++". The negative control sections were scored as "0" and the intense immunostaining in distal convoluted tubules of rat kidney were scored as "+++" as the positive controls (see Table 1).

2.2. Western blot

2.2.1. Tissue preparation

Samples of mandibular condyles from three other growing (1–1.5 kg) and three other adult male rabbits (4–4.5 kg) were used for Western blot and slot blot. The condyles were dissected free as quickly as possible under anaesthesia, as described above. They were cut sagittally under the microscope and tiny fragments containing only cartilage were quick frozen in liquid nitrogen and kept frozen at −70°C until used.

2.2.2. SDS–PAGE

The frozen fragments of condyles were placed in 200 μl of PBS (pH 7.4). The fragments were homogenized on ice with an Omni 1000 tissue grinder (Omni International, Waterbury, CT) for 1 min. A 200-μl sample of each homogenate was placed in 200 μl of a 2× homogenization solution (50 mM Tris base, pH 7.4, 2% SDS, 5 mM benzamidine, 10 μg/ml trypsin inhibitor, 2.5 μM leupeptin and 1.5 μM pepstatin A). Homogenate samples (5 μl) were used for the bicinchoninic protein assay (Pierce Laboratories, Rockford, IL).

Each homogenate sample (50 μl) was freeze-dried at −35°C under vacuum and combined with 1× sample buffer solution (50 mM Tris–HCl, pH 6.8, containing 5% β-mercaptoethanol, 2% SDS, 10% glycerol, and 0.1% bromophenol blue). Samples containing equal protein concentrations (1.66 μg/μl) were denatured by heating in a boiling water bath (100°C) for 5 min. Samples (20 μg) of biotinylated marker proteins of known molecular weight (Bio-Rad, Richmond, CA) were also treated in a similar manner.

Portions (50 μg) of each protein sample were placed in wells of 7% SDS–polyacrylamide gels prepared by the method of Laemmli (1970). Gel electrophoresis was initiated at 200 V and continued for 45 min. After electrophoresis, proteins were transferred from the gels to nitrocellulose using a transblot apparatus (Bio-Rad) at 100 V for 1 h by the electroblotting technique of Towbin et al. (1979). The relative migration of proteins in each homogenate was compared with the migration of marker proteins to determine the molecular weight of each band.

2.2.3. Immunochemical staining of Western blots

Proteins immobilized on nitrocellulose were stained with the monoclonal antibody 5F10 directed against the human erythrocyte Ca^{2+} pump by the avidin–biotin immunoperoxidase method, similar to the technique used for the immunohistochemistry described above.

After rinsing with PBS containing 0.05% Tween 20 (Sigma) (PBS–Tween), nitrocellulose blots were incubated in 3% hydrogen peroxide in PBS–Tween for 5 min to block endogenous peroxidase activity, and rinsed three times for 3 min each with additional PBS–Tween. A total of 10 mg/ml bovine serum albumin in PBS was applied for 1 h to block non-specific binding of antibodies. While incubating, two drops of 0.1%

sodium azide were added to the blots to inhibit bacterial catalase. Without rinsing, a 1:750 dilution of 5F10 antibody in PBS–Tween was allowed to react with the blots at room temperature for 1 h. After washing in PBS–Tween, the biotinylated horse anti-mouse IgG (1:200) was layered over immobilized proteins on the blots for 30 min at room temperature. After washing in PBS–Tween, the blots were incubated for 30 min in the same avidin–peroxidase complex described above for immunohistochemistry. After washing in PBS–Tween, 0.05 M DAB in 0.03% H_2O_2 was applied as the substrate for the peroxidase. The colour change on the blots was monitored visually and the reaction stopped with sterile water. DAB reacts with reduced H_2O_2 to yield a brown-coloured reaction product over protein bands where the primary antibody binds.

The molecular weights of proteins transferred to nitrocellulose were determined by calculating the migration of the protein bands relative to biotinylated marker proteins of known molecular weight. These biotinylated marker proteins also react with the avidin–peroxidase complex.

2.2.4. Slot blot

Portions (10 μg) of each protein sample were mixed with 10 μl of 2× slot-blot buffer solution (10 mM Tris base, 4% SDS and 0.05% β-mercaptoethanol). Proteins were denatured by heating for 5 min in a boiling water bath before loading in wells of a slot-blot apparatus and immobilizing on nitrocellulose. The blots were stained with antibody 5F10 by the same protocol as previously described for the Western blot.

Stained blots were analysed by densitometry on a Hoefer GS 300 scanning densitometer (Hoefer Scientific Instruments, San Francisco, CA) which included a Hoefer GS 365W electrophoresis data-reduction system. Scanning densitometry of the blots provided peak areas for each sample. The peak areas were expressed as the mean of stain intensity for each sample, in absorbency units (AU) per mm. The areas under the peaks were integrated for comparison of the amounts of Ca^{2+}-pump epitope in cartilage from growing and adult rabbits.

3. Results

3.1. Light-microscopic immunohistochemistry

Photomicrographs of haematoxylin-and-eosin stained sections of growing (Plate 1) and adult (Plate 1.2) condyles show the basic architecture of the condyle. The various cell layers are all labelled for comparison with the tissues incubated with Ca^{2+}-pump antibody 5F10.

Table 1
Summary of immunocytochemical localization of Ca^{2+}-pump epitope in the rabbit mandibular condyle[a]

Cartilage	Growing ($n = 3$)	Adult ($n = 3$)
Fibrous layer	0	0
Reserve cell zone	+	0 or +
Flat chondrocytes	+	+
Upper hypertrophic cell zone	+ + +	+ + +
Lower hypertrophic cell zone	+	0
Subchondral bone	**Growing**	**Adult**
Osteoblasts	+ + +	+ + +
Osteoclasts or chondroclasts	+ + +	+ + +
Osteocytes	0	0

[a] 0, no immunostaining. +, mild immunostaining of a few cells. + +, moderate immunostaining of most cells. + + +, strong immunostaining of most cells.

Positive control sections of rat kidney incubated with 5F10 showed immunoperoxidase staining in the distal convoluted tubules as expected (Borke et al., 1989) (not shown). Negative control sections of the mandibular condyles, which were not incubated with the monoclonal antibody, showed no immunoperoxidase staining in any cell zones in either growing or adult rabbits (Plate 1.3, 1.5, 1.7, 1.9).

Higher-magnification photomicrographs of the experimental sections showed that immunostaining with 5F10 was absent from the fibrous layer, including the articular and polymorphic cell zones, of the growing and adult condyles. A weak immunoperoxidase reaction was first detected in a few cells at the bottom of the reserve cell zone and in the membranes of flat chondrocytes (Plate 1.4, 1.6) by comparison with negative control sections (Plate 1.3, 1.5).

As the maturation of chondrocytes progressed in the upper and middle hypertrophic cell zone, the immunoreaction with 5F10 in the hypertrophic cells became stronger (Plate 1.8, 1.10). The Ca^{2+}-pump epitopes in the hypertrophic chondrocytes appeared to be clear and asymmetrically distributed in their plasma membranes (Plate 1.8).

The immunoreaction was very strong in the middle portion of the hypertrophic cell layer and rapidly disappeared in the lower hypertrophic cell zone of both the growing and adult condyles (Plate 1.8, 1.10). A few hypertrophic chondrocytes of the growing condyles, still showed a weak reaction, although most cells were apoptotic and surrounded by calcified matrix invaded by vessels, and by osteoclasts or chondroclasts near the sites of resorption (Plate 1.11, 1.12).

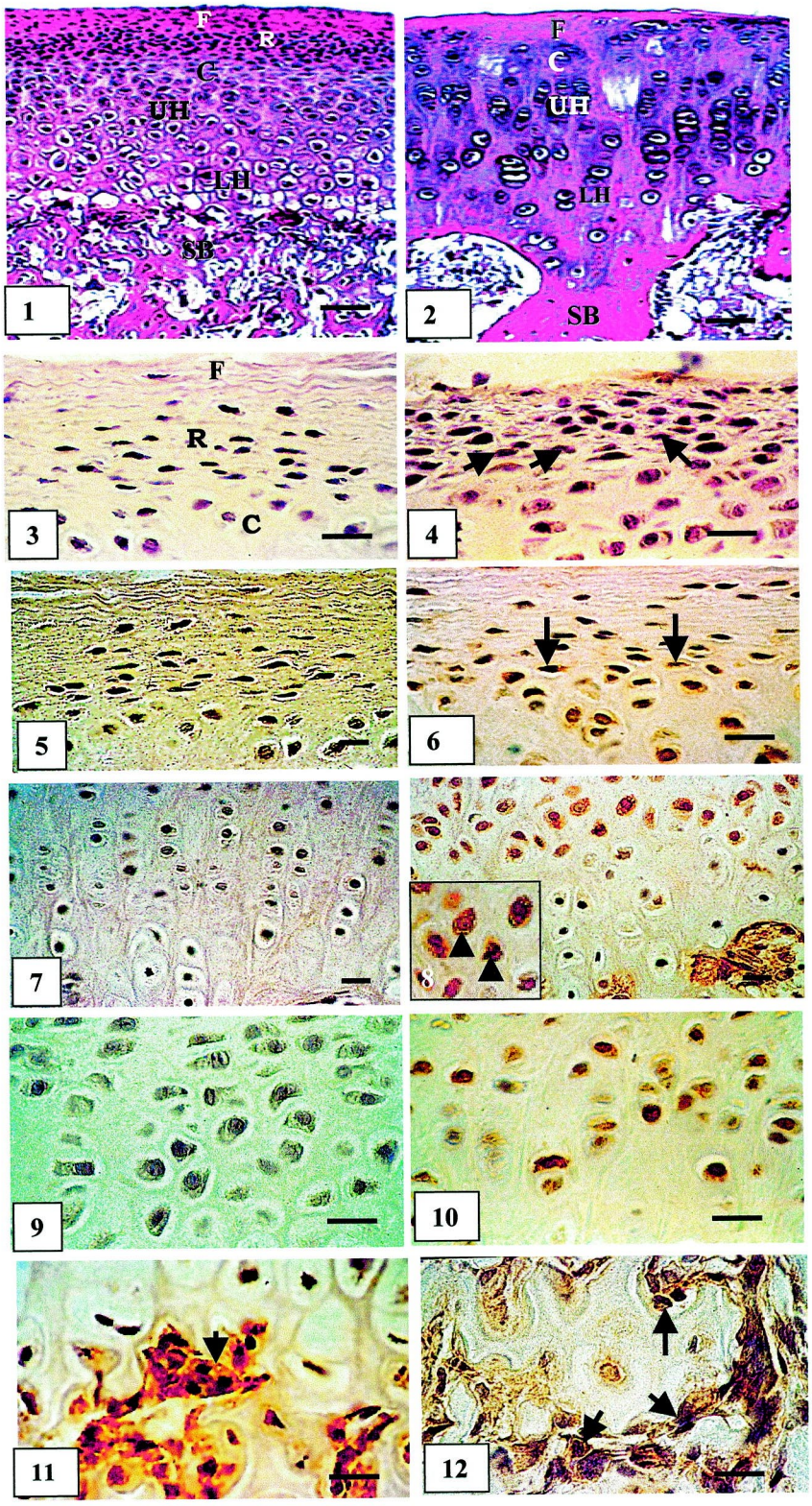

Plate 1. (*Caption overleaf on p. 242*).

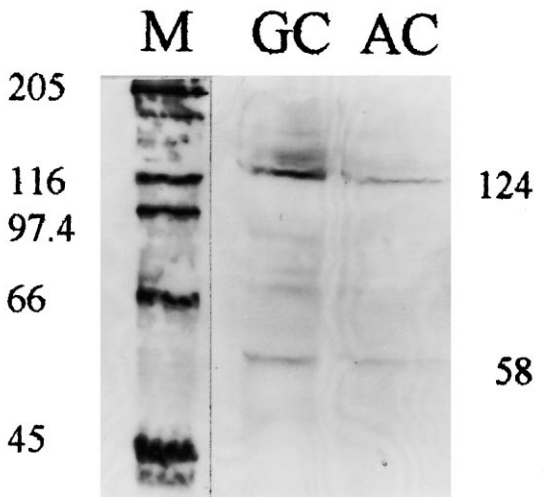

Fig. 1. Western blot analysis of tissue homogenates from growing and adult rabbit mandibular condyle with monoclonal antibody 5F10 after 7% SDS–PAGE: adult condylar cartilage (AC), growing condylar cartilage (GC). Note the prominent band at 124 kDa and additional band at 58 kDa.

In the provisional calcified zone of cartilage and subchondral bone, a strong positive reaction with the antibody 5F10 was found in osteoblasts, osteoclasts and chondroclasts but no such reaction was found in osteocytes (Plate 1.11, 1.12).

3.2. Western blot

Western blotting of homogenates of cartilage from growing as well as adult rabbits showed binding of antibody 5F10 to major bands of 124 kDa (Fig. 1). Monoclonal antibody 5F10 also reacted with additional major bands around 58 kDa.

Immunoperoxidase staining with monoclonal antibody 5F10 appeared more intense in bands of cartilage from growing rabbits than in those of adult rabbits, although the same amounts of each protein were applied.

Table 2
Integrated peak areas of the adult and growing condylar cartilage (AU/mm)

Cartilage	Mean ± SE
Adult condylar ($n = 3$)	1054 ± 172
Growing condylar ($n = 3$)	2266 ± 231 ($p < 0.05$)

3.3. Slot blot

Slot blotting of cartilage homogenates taken from growing and adult rabbits showed immunoperoxidase staining of variable intensity over areas of protein immobilized on nitrocellulose. Scanning densitometry of the blots provided peaks corresponding to the density of the 5F10 binding. The integrated peak areas corresponding to the amounts of Ca^{2+}-pump protein present in each sample were calculated. The amounts of Ca^{2+}-pump epitopes of growing cartilage (2266 ± 399 SD AU/mm) were more than twice as much as that of adult cartilage (1054 ± 298 SD AU/mm) (Table 2).

4. Discussion

Plasma-membrane Ca^{2+}–Mg^{2+} ATPases are found

Plate. 1. (1.1) Articular portion of young rabbit mandibular condyle illustrating the fibrous layer (F), the reserve cell layer (R), the chondrocytic layer (C), the upper hypertrophic layer (UH), the lower hypertrophic layer (LH), and subchondral bone (SB). H&E stain. Bar = 100 μm. (1.2) Adult rabbit mandibular condylar cartilage illustrating the fibrous layer (F), thin chondrocytic layer (C), the upper hypertrophic layer (UH), the lower hypertrophic layer (LH), and subchondral bone (SB). Note the organization of the hypertrophic cells into vertical columns, lesser cellularity of the cartilage, and the decline in the number of the reserve cells when compared to the young condylar cartilage (1.1). H&E stain. Bar = 100 μm. (1.3) Negative control section of the growing rabbit mandibular condyle incubated without 5F10 illustrating the absence of immunostaining in the fibrous (F), reserve cell layer (R), and chondrocytic layer (C). Bar = 30 μm. (1.4) Section of growing rabbit condylar cartilage incubated with 5F10. Note the weak immunostaining of cells of the reserve cell layer (arrows). Bar = 50 μm. (1.5) Negative control section of adult rabbit mandibular condyle incubated without 5F10. Note the absence of immunostaining in all layers. Bar = 30 μm. (1.6) Section of adult rabbit mandibular condyle incubated with 5F10. Note the absence of immunostaining in the fibrous layer and the weak immunostaining of the reserve cell layer (arrows). Bar = 30 μm. (1.7) Negative control section of young condyle incubated without 5F10; note the absence of immunostaining. Bar = 50 μm. (1.8) Section of young condyle incubated with 5F10. Note the strong immunostaining in the upper hypertrophic layer. Higher magnification (insert) showing the immunostaining localized at the cell membrane (arrowhead). Bar = 50 μm. (1.9) Negative control section of adult condyle; note the absence of immunostaining. Bar = 30 μm. (1.10) Section of adult condyle incubated with 5F10 illustrating strong immunostaining in the upper hypertrophic layer and its absence from the lower hypertrophic cell layer. Bar = 30 μm. (1.11) Section of growing condyle incubated with 5F10 illustrating strong immunostaining of bone marrow osteclast (arrow). Bar = 30 μm. (1.12) Section of growing condyle incubated with 5F10; note the strong immunostaining of the osteoblasts of the subchondral bone (arrows). Bar = 30 μm.

in most eukaryotic cells and are part of the mechanism required to maintain intracellular Ca^{2+} homeostasis (Carafoli, 1987). In addition to this "housekeeping" function, these ATPases also help to move large amounts of Ca^{2+} across tissues that transport Ca^{2+} and into tissue environments that mineralize (Zanetti et al., 1982; Akisaka and Gay, 1985).

In the present study, a monoclonal antibody (5F10) directed against human erythrocyte plasma-membrane Ca^{2+}–Mg^{2+} ATPase (Borke et al., 1989) was used to localize the Ca^{2+} pump in plasma membranes of cells of the rabbit mandibular condyle. Localization of Ca^{2+} ATPase by measuring its activity sometimes leads to confusion associated with reaction products either from ecto-ATPases or membrane phosphatases, which may confound measurements of the Ca^{2+}–Mg^{2+} ATPase associated with Ca^{2+} transport (Stahl and Baskin, 1990). The use of a specific antibody prepared against the plasma membrane Ca^{2+}-pumping Ca^{2+}–Mg^{2+} ATPase is therefore useful in separating these enzymes.

Our immunohistochemical findings demonstrate asymmetrically distributed Ca^{2+}-pump epitopes in the plasma membranes and cytoplasm of hypertrophic chondrocytes in both growing and adult rabbit mandibular condyles. Cytoplasmic staining may represent the localization of precursors of the Ca^{2+}-pump protein or may represent tangential sections of plasma membrane seen due to the thickness of the tissue sections. As expected from previous studies (Borke et al., 1988; Akisaka et al., 1988), the Ca^{2+}–Mg^{2+} ATPase (Ca^{2+} pump) epitopes were also found in the plasma membranes of osteoblasts and osteoclasts. On the other hand, no such epitopes were detected in the perichondrium of the condyles, including the articular zone, the polymorphic cell zone and the proliferative cell zone.

The growing rabbit condyles showed specificity for the Ca^{2+}-pump epitopes in the hypertrophic cell zone. Specific localization of the epitopes was exclusively seen in the upper and middle hypertrophic cell zone. In the same zone, mitochondria of chondrocytes reportedly start releasing their accumulated calcium or calcium phosphate granules into matrix vesicles located in the extracellular matrix (Brighton and Hunt, 1974; Ali, 1976).

The mitochondrial granules are postulated to be amorphous calcium phosphate complexes and are extruded out of the cell via an outpocketing process of reverse phagocytosis (Lehninger, 1977). The exact mechanisms of extrusion of mitochondrial granules and initial nucleation of apaptite in the matrix are obscure. It can be postulated that mitochondrial Ca^{2+} may also be released from the cell by the plasma-membrane Ca^{2+} pump, as the precipitation of amorphous calcium phosphate is thought to be an easily reversible process (Lehninger, 1977).

The Ca^{2+}-pump epitopes were sometimes seen in the lower hypertrophic cell zone of growing condyles where most surrounding cells appear to have degenerated and also appear to have been "attacked" by invading capillaries (Plate 1.10). This is somewhat surprising as this zone is considered to be devoid of nutrition and oxygen (Wuthier, 1982). In addition, in adult rabbits, Ca^{2+}-pump epitopes were found in hypertrophic chondrocytes surrounded by rather eosinophilic, calcified matrix substances (Plate 1.10). These findings suggest a continuous Ca^{2+} transport by the hypertrophic chondrocytes into specific sites of the matrix until they are eliminated by vascular invasion.

Recent studies have shown that all hypertrophic chondrocytes, including terminal cells, possess intact cellular membranes, nuclei and intracellular organelles. This suggests that rather than going through a programmed degeneration, the surviving cells may play an active part at the mineralization front (Cowell et al., 1987; Hunzinker, 1994). Therefore, the presented data suggested that, in addition to regulating intracellular Ca^{2+} homeostasis, a Ca^{2+}–Mg^{2+} ATPase pump in hypertrophic chondrocytes might be associated with the efflux of mitochondrial Ca^{2+} and regulate Ca^{2+} transport to the initial calcification front in the extracellular matrix of condyle cartilage.

Western blotting of freeze-dried homogenates of cartilage from growing and adult rabbit condyles demonstrated major bands of 124 kDa (Fig. 1), slightly lower than those of Ca^{2+} pumps previously described (130–145 kDa) (Carafoli, 1991). The present study may not show binding of antibody 5F10 to intact Ca^{2+}-pump protein, probably because of either proteloysis during tissue processing or high endogenous protease activity. That activity is suggested by the cellular degeneration seen in both the lower hypertrophic cell zone and zone of vascular invasion where cellular fragmentation (and presumably, protein fragmentation) is observed in tissue sections. Thus, the bands between 124 kDa, as well as additional bands around 58 kDa, are likely to represent proteolytic fragments of the intact Ca^{2+} pump. Results of studies of bands associated with the limited proteolysis of the Ca^{2+} pump are consistent with this assertion (Zurini et al., 1984; Zvaritch et al., 1990).

Slot blotting showed that growing condylar cartilage contains more plasma-membrane Ca^{2+}-pump protein relative to total cellular protein than adult cartilage. This result suggests that the additional Ca^{2+}-pump molecules promote a more active movement of Ca^{2+} out of cells in the growing rabbit than in the adult rabbit.

A study by Wang et al. (1997) suggests that the proto-oncogene *Bcl-2* may protect chondrocytes until after mineralization has occurred by inhibiting the

action of the apoptosis inducer, Bax. Their study demonstrated a progressive decrease in *Bcl-2* with cartilage maturation while showing a consistent amount of Bax at all stages. The demonstrated presence of the Ca^{2+} pump in the hypertrophic chondrocytes is consistent with the timeframe for the maturation of the chondrocyte. This timeframe includes the initial nucleation process, which is known to involve mitochondria and the activity of matrix vesicles, prior to cartilage calcification and the terminal maturation of the cells and apoptosis. In addition to maintaining intracellular Ca^{2+} homeostasis, our data suggest that the plasma-membrane Ca^{2+} pump of the hypertrophic chondrocytes may play a part in the initial phase of biological cartilage calcification in the mandibular condyle.

Acknowledgements

We wish to thank Ms. Cathy Pennington and Ms. Vera Larke for their invaluable technical assistance and Ms. Michelle Burnside for typing the manuscript.

References

Akisaka, T., Gay, C.V., 1985. Ultrastructural localization of calcium-activated adenosine triphosphatase (Ca^{2+}-ATPase) in growth-plate cartilage. Journal of Histochemistry and Cytochemistry 33, 925–932.

Akisaka, T., Kawaguchi, H., Subita, G.M., Shigenaga, Y., Gay, C.V., 1988. Ultrastructure of matrix vesicles in chick growth plate as revealed by quick freezing and freeze substitution. Calcified Tissue International 42, 383–393.

Ali, S.Y., 1976. Analysis of matrix vesicles and their role in the calcification of epiphyseal cartilage. Federation Proceedings 35, 135–142.

Anderson, H.C., 1992. Conference introduction and summary. Bone and Mineral 17, 107–112.

Balmain, N., Hotton, D., Cuisinier-Gleizes, P., Mathieu, H., 1989. Immunoreactive calbindin-D9 K localization in matrix vesicle-initiated calcification in rat epiphyseal cartilage: an immunoelectron microscope study. Journal of Bone and Mineral Research 4, 565–575.

Balmain, N., Hauchecorne, M., Pike, J.W., Cuisinier-Gleizes, P., Mathieu, H., 1993. Distribution and subcellular immunolocalization of 1,25 dihydroxyvitamin D3 receptors in rat epiphyseal cartilage. Cell and Molecular Biology 36, 339–350.

Borke, J.L., Eriksen, E.F., Minami, J., Keeting, P., Mann, K.G., Penniston, J.T., Riggs, B.L., Kumar, R., 1988. Epitopes of the human erythrocyte Ca^{2+}-Mg^{2+} ATPase pump in human osteoblast-like cell plasma membranes. Journal of Clinical Endocrinology and Metabolism 67, 1299–1304.

Borke, J.L., Caride, A., Verma, A.K., Penniston, J.T., Kumar, R., 1989. Plasma membrane calcium pump and 28-kDa calcium binding protein in cells of rat kidney distal tubules. American Journal of Physiology 257, F842–F849.

Brighton, C.T., Hunt, R.M., 1974. Mitochondrial calcium and its role in calcification. Histochemical localization of calcium in electron micrographs of the epiphyseal growth plate with K-pyroantimonate. Clinical Orthopaedics and Related Research 100, 406–416.

Carafoli, E., 1987. Intracellular calcium homeostasis. Annual Review of Biochemistry 56, 395–433.

Carfoli, E., 1991. Calcium pump of the plasma membrane. Physiological Review 71, 129–153.

Cowell, H.R., Hunziker, E.B., Rosenberg, L., 1987. The role of hypertrophic chondrocytes in endochondral ossification and in the development of secondary centers of ossification. Journal of Bone and Joint Surgery 69A, 159–161.

Gunter, T.E., Zuscik, M.J., Puzas, J.E., Gunter, K.K., Rosier, R.N., 1990. Cytosolic free calcium concentrations in avian growth plate chondrocytes. Cell Calcium 11, 445–457.

Hsu, S., Raine, L., Fanger, H., 1981. Use of avidin-biotin-peroxidase complex (ABC) in immunoperoxidase techniques: a comparison between ABC and unlabeled antibody (PAP) procedures. Journal of Histochemistry and Cytochemistry 29, 577.

Hunziker, E.B., 1994. Mechanism of longitudinal bone growth and its regulation by growth plate chondrocytes. Microscopy Research and Technology 28, 505–519.

Ianotti, J.P., Brighton, C.T., Stambough, J.L., Storey, B.T., 1985. Calcium flux and endogenous calcium content in isolated mammalian growth-plate chondrocytes, hyaline-cartilage chondrocytes, and hepatocytes. Journal of Bone and Joint Surgery 67, 113–120.

Laemmli, U.K., 1970. Cleavage of structural proteins during the assembly of the head of bacteriophage T4. Nature 227, 680.

Lehninger, A.L., 1977. Mitochondria and biological mineralization processes. An exploration. Horizons in Biochemistry and Biophysics 4, 1–30.

Lehninger, A.L., 1978. Transport and accumulation of calcium in mitochondria. Annals of the New York Academy of Sciences 307, 160–176.

Matthews, J.L., Martin, J.H., 1971. Intracellular transport of calcium and its relationship to the homeostasis and mineralization. An electron microscope study. American Journal of Medicine 50, 589–597.

Moy, T.C., Walters, J.R.F., Weisner, M.W., 1986. Intestinal basolateral membrane Ca^{2+}-ATPase activity with properties distinct from those of the Ca^{2+} pump. Biochemical and Biophysical Research Communications 141, 979.

Stahl, W.L., Baskin, D.G., 1990. Histochemistry of ATPases. Journal of Histochemistry and Cytochemistry 38, 1099–1122.

Ten Cate, A.R., 1998. Oral Histology, 5th ed. Mosby-Year Book, St. Louis, pp. 105–127.

Towbin, H., Staehlin, T., Gordon, J., 1979. Electrophoretic transfer of proteins from polyacrylamide gels to nitrocellulose sheets. Proceedings of the National Academy of Sciences of the United States of America 76, 4350.

Wang, Y., Toury, R., Hauchecorne, M., Balmaine, N., 1997. Expression of Bcl-2 protein in the epiphyseal plate cartilage and trabecular bone of growning rats. Histochemistry and Cell Biology 108, 45–55.

Wuthier, R.E., 1982. A review of the primary mechanism of endochondral calcification with special emphasis on the role of cells, mitochondria and matrix vesicles. Clinical Orthopaedics and Related Research 169, 219.

Zanetti, M., Camerotto, R., Romeo, D., de Bernard, B., 1982. Active extrusion of Ca^{2+} from epiphyseal chondrocytes of normal and rachitic chickens. Biochemical Journal 202, 303–307.

Zurini, M., Krebs, J., Penniston, J.T., Carafoli, E., 1984. Controlled proteolysis of the purified Ca^{2+}-ATPase of the erythrocyte membrane. A correlation between the structure and the function of the enzyme. Journal of Biological Chemistry 259, 618–627.

Zvaritch, E., James, P., Vorherr, T., Falchetto, R., Modyanov, N., Carafoli, E., 1990. Mapping of functional domains in the plasma membrane Ca^{2+} pump using trypsin proteolysis. Biochemistry 29, 8070–8076.